Reach of Fermilab Tevatron upgrades in gauge-mediated supersymmetry breaking models

Howard Baer,[1] P. G. Mercadante,[2] Xerxes Tata,[2] and Yili Wang[2]
[1]*Department of Physics, Florida State University, Tallahassee, Florida 32306*
[2]*Department of Physics and Astronomy, University of Hawaii, Honolulu, Hawaii 96822*
(Received 15 March 1999; published 14 July 1999)

We examine signals for sparticle production at the Fermilab Tevatron within the framework of gauge-mediated supersymmetry breaking models for four different model lines, each of which leads to qualitatively different signatures. We identify cuts to enhance the signal above standard model backgrounds, and use ISAJET to evaluate the supersymmetry reach of experiments at the Fermilab Main Injector and at the proposed TeV33. For the model lines that we have examined, we find that the reach is at least as large, and frequently larger, than in the minimal supergravity framework. For two of these model lines, we find that the ability to identify b-quarks and τ-leptons with high efficiency and purity is essential for the detection of the signal.
[S0556-2821(99)03615-2]

PACS number(s): 14.80.Ly, 11.30.Pb, 12.60.Jv, 13.85.Qk

I. INTRODUCTION

Models where gauge interactions [1,2] rather than gravity serve as messengers of supersymmetry breaking have been the focus of many recent phenomenological analyses [3–15] of supersymmetry (SUSY). In these models, sparticle masses and decay patterns differ from those in the extensively studied minimal supergravity (MSUGRA) model [16] which has served as the framework for many experimental analyses of supersymmetry. Perhaps the most important difference between the MSUGRA framework and gauge-mediated SUSY breaking (GMSB) models with a low SUSY breaking scale is the identity of the lightest SUSY particle (LSP). In the former case, the lightest neutralino ($\tilde{Z}_1$) is almost always the LSP, while in the GMSB framework, the gravitino is much lighter than other sparticles. Moreover, while the gravitino is essentially decoupled in MSUGRA scenarios, the couplings of the Goldstino (which forms the longitudinal components of the massive gravitino), though much smaller than gauge couplings, may, nonetheless, be relevant for collider physics in that they can cause the next to lightest SUSY particle (NLSP) to decay into a gravitino *inside the detector*. The precise decay pattern and lifetime of the NLSP depends on its identity and on model parameters. For instance, if $\tilde{Z}_1$ is the NLSP, it would decay via $\tilde{Z}_1 \to \tilde{G} + \gamma$, and if kinematically allowed, also via $\tilde{Z}_1 \to \tilde{G} + Z$, or into the various Higgs bosons of SUSY models via $\tilde{Z}_1 \to \tilde{G} + h$, H, or A. If, on the other hand, the NLSP is a slepton, it would decay via $\tilde{l} \to \tilde{G} + l$, etc. Sparticles other than the NLSP decay only very rarely to gravitinos, so that it is safe to neglect these decays in any analysis. Thus heavier sparticles cascade decay as usual to the NLSP, which then decays into the gravitino as described above.

Sparticle signatures differ from those in the MSUGRA framework for two basic reasons. First, if the NLSP is not the lightest neutralino, the cascade decay patterns to the NLSP are modified. Second, the NLSP (which need not be electrically neutral) itself decays into a gravitino and standard model (SM) particles. The gravitinos escape the experimental apparatus undetected resulting in $\not{E}_T$ in SUSY events. In the GMSB framework, however, neutralino NLSP decays may also result in isolated photons or Z or Higgs bosons which could provide additional handles to reduce SM backgrounds to the SUSY signal. If the NLSP is a slepton, all SUSY events should contain leptons of the same flavor as the slepton NLSP in addition to $\not{E}_T$. While it may be possible to have other candidates for the NLSP, this does not seem to be the case in the simplest realizations of the GMSB framework, and we will not consider this possibility any further.

Within the minimal GMSB (MGMSB) framework, supersymmetry breaking in a hidden sector is communicated to the observable sector via SM gauge interactions of messenger particles [with quantum numbers of $SU(2)$ doublet quarks and leptons] whose mass scale is characterized by M. As a result, the soft SUSY breaking masses induced for the various sparticles are directly proportional to the strength of their gauge interactions. Thus, colored squarks are heavier than sleptons, and gluinos are heavier than electroweak gauginos. The observable sector sparticle masses and couplings are determined (at the scale M) by the GMSB model parameter set:

$$\Lambda, M, n_5, \tan\beta, \mathrm{sgn}(\mu), C_{grav}. \tag{1.1}$$

Of these, Λ is the most important parameter in that it sets the scale of sparticle masses. The model predictions for the mass parameters at the scale M are then evolved down to the sparticle mass scale via renormalization group evolution (RGE). Radiative breaking of electroweak symmetry determines $|\mu|$. The weak scale SUSY parameters depend only weakly on the messenger mass scale M, since this primarily enters as the scale at which the mass relations predicted by the model are assumed to be valid. There is an additional dependence of the sparticle spectrum on M due to threshold effects [17], but this is also weak as long as M/Λ is not very close to unity. Messenger quarks and lepton, it is assumed, can be classified into complete vector representations of $SU(5)$: the number (n_5) of such multiplets is required to be $\leqslant 4$ for the messenger scale $M = \mathcal{O}(100\ \mathrm{TeV})$ in order that the gauge couplings remain perturbative up to the grand unification

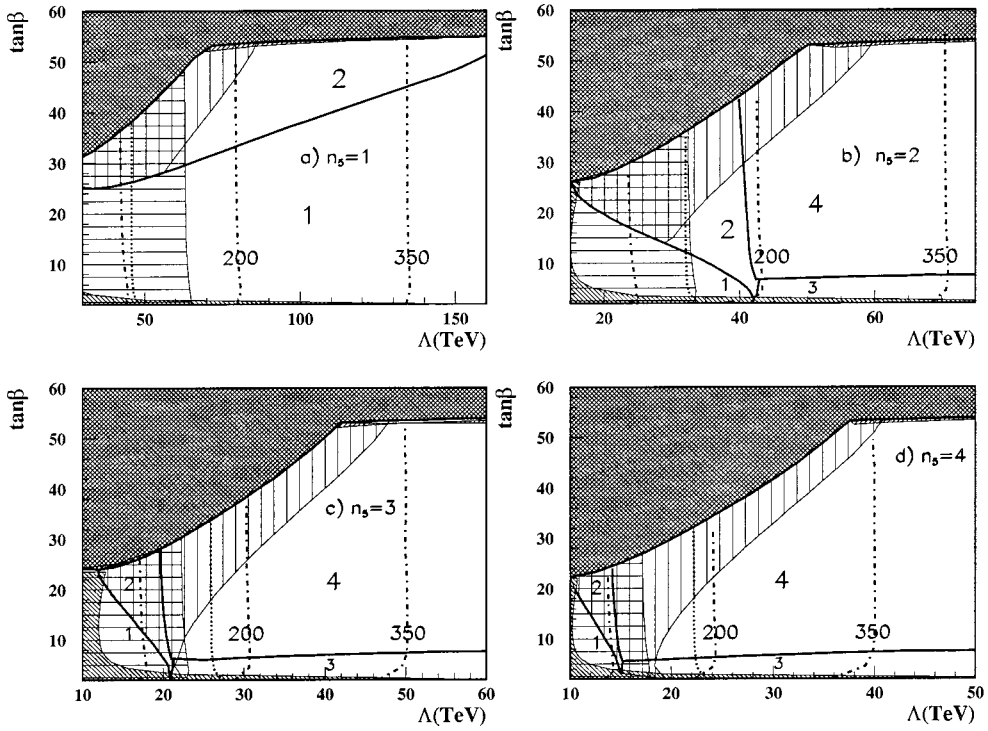

FIG. 1. The four regions of the Λ-tan β parameter plane discussed in Sec. I of the text. We fix $M=3\Lambda$, and take μ to be positive. The heavy solid lines denote the boundaries between these regions. The grey region is excluded because electroweak symmetry is not correctly broken. The shaded regions should be probed by experiments at LEP and are nearly excluded because $m_{\tilde{\tau}}\leqslant 76$ GeV (vertical shading), $\tilde{Z}_1\leqslant 84$ GeV (horizontal shading) or $m_h\leqslant 95$ GeV (or $m_A\leqslant 83$ GeV) (diagonal shading). The dot-dashed contours are where the chargino mass is 95, 200 or 350 GeV, while the dotted line is the contour of $m_{\tilde{e}_1}=90$ GeV.

scale. Finally, the parameter $C_{grav}\geqslant 1$ [13] (essentially, the ratio of hidden sector to messenger sector SUSY breaking vevs) can be used to dial the gravitino mass beyond its minimum value. Effectively, C_{grav} parametrizes the rate for sparticle decays into a gravitino. This decay is most rapid when $C_{grav}=1$, while for larger values of C_{grav}, the NLSP may decay with an observable decay vertex, or may even be sufficiently long-lived to pass all the way through the detector. In this extreme case, SUSY event topologies would be identical to those in the MSUGRA model if $\tilde{Z}_1$ is the NLSP. However, for the case where a charged slepton is the NLSP, SUSY events would necessarily contain a pair of penetrating tracks from the long-lived slepton NLSP, which might be detectable at the Fermilab Tevatron as ''additional (possibly slow) muons'' [11,14]. In our analysis, we assume that the NLSP decays promptly and fix $C_{grav}=1$; i.e., we do not attempt to model the additional handle displaced vertices might provide to reduce SM backgrounds.

Many of the phenomenological implications depend only weakly on the parameter M. Thus, the Λ-tan β plane provides a convenient panorama for illustrating the diversity of phenomenological possibilities in GMSB scenarios. This is shown in Fig. 1 for $M=3\Lambda$ and (*a*) $n_5=1$, (*b*) $n_5=2$, (*c*) $n_5=3$, and (*d*) $n_5=4$. We choose μ to be positive, since for this choice, the model predictions [6,18] are well within experimental constraints [19] from the decay $b\rightarrow s\gamma$ over essentially the whole plane. In region 1 in Fig. 1(a)–1(d) (the boundaries of these regions are the heavy solid lines), the lightest neutralino is the NLSP, so that $\tilde{Z}_1\rightarrow\tilde{G}\gamma$ (and to Z and Higgs bosons if these decays are kinematically allowed). In region 2, $m_{\tilde{\tau}_1}<m_{\tilde{Z}_1}$, while other sleptons are heavier than $\tilde{Z}_1$, and cascade decays of sparticles terminate in $\tilde{\tau}_1$, except immediately above the boundary between regions 1 and 2 where the decay $\tilde{Z}_1\rightarrow\tilde{\tau}_1\tau$ is kinematically forbidden. For parameters in region 2, we thus expect an excess of τ leptons in SUSY events [9]. In regions 3 and 4 in Fig. 1(b)–1(d), not only $\tilde{\tau}_1$, but also $\tilde{e}_1\simeq\tilde{e}_R$ and $\tilde{\mu}_1\simeq\tilde{\mu}_R$, are lighter than $\tilde{Z}_1$. Thus neutralinos are effectively sources of real (dominantly right-handed) sleptons. In region 3, $\tilde{l}_1\rightarrow l\tilde{G}$ because its decay $\tilde{l}_1\rightarrow\tilde{\tau}_1\tau l$ $(l=e,\mu)$ is kinematically forbidden. The decay $\tilde{\mu}_1\rightarrow\nu_\mu\tilde{\tau}_1\nu_\tau$ which occurs via suppressed muon Yukawa couplings is kinematically allowed, and may compete with the decay to $\tilde{\mu}_1\rightarrow\mu\tilde{G}$; for $C_{grav}=1$, we find that this decay (which has been included in our computation), is unimportant. In region 4, the decays $\tilde{l}_1\rightarrow\tilde{\tau}_1\bar{\tau}l$ and $\tilde{l}_1\rightarrow\bar{\tilde{\tau}}_1\tau l$ are also allowed, and compete with the gravitino decay of $\tilde{l}_1$. Frequently, the stau decays of $\tilde{l}_1$ dominate its decays to gravitino, and then, as for region 2, SUSY events will be characterized by an abundance of taus in the final state. Signals from sparticle production will clearly depend on which of these regions the model parameters happen to lie.

The gray regions in Fig. 1 are excluded because the observed pattern of electroweak symmetry breaking is not ob-

tained: in the wedge in the upper left corner, $m^2_{\tilde{\tau}_R} < 0$, while in the band on top, $m_A^2 < 0$. The non-observation of sparticle signatures in experiments at the CERN e^+e^- collider LEP excludes other portions of the plane. Within the minimal supersymmetric standard model (MSSM) charginos have been excluded if $m_{\tilde{W}_1} \leqslant 90$–$95$ GeV. While this limit has been obtained assuming that charginos and selectrons decay into a stable neutralino which escapes detection, we expect that an even more striking signature is obtained if $\tilde{Z}_1$ decays via $\tilde{Z}_1 \to \gamma \tilde{G}$. The leftmost dot-dashed line in Fig. 1 is the contour $m_{\tilde{W}_1} = 95$ GeV: to its left, charginos are lighter than 95 GeV. To assist the reader in assessing the sparticle mass scale, we have also shown mass contours for $m_{\tilde{W}_1} = 200$ GeV and $m_{\tilde{W}_1} = 350$ GeV. MSSM searches for acollinear electron pairs exclude selectrons lighter than about 90 GeV. This limit should certainly be valid within this framework if $\tilde{e}_1 \to \tilde{G} e$ (region 3) or even if it decays to $\tilde{Z}_1$ that subsequently decays to a photon (region 1). The dotted line is the contour $m_{\tilde{e}_1} = 90$ GeV. For the case where $\tilde{e}_1$ mainly decays to $\tilde{\tau}_1$, the actual bound may be somewhat weaker, and closer to the MSSM stau bound ~ 76 GeV. The most stringent experimental limit for the $n_5 = 1$ and $n_5 = 2$ cases in frames (*a*) and (*b*) comes from the the LEP search [20] for $\gamma\gamma + \not{E}_T$ events from $e^+e^- \to \tilde{Z}_1\tilde{Z}_1$ production. The cross section for this process depends on the selectron mass. The ALEPH analysis [20] for $n_5 = 1$ results in the lower limit, $m_{\tilde{Z}_1} \geqslant 84$ GeV [21]. For larger values of n_5, the selectron to $\tilde{Z}_1$ mass ratio is smaller, so that the corresponding cross section is even larger than in the $n_5 = 1$ case. Indeed the DELPHI Collaboration [20] has obtained a preliminary bound $m_{\tilde{Z}_1} \gtrsim 88$ GeV for $n_5 = 2$, for parameters in region 1. If $m_{\tilde{\tau}_1} \leqslant m_{\tilde{Z}_1}$, $\tilde{Z}_1$s act as sources of staus and add to the signal from direct stau pair production. The DELPHI search for acollinear tau pairs still limits $m_{\tilde{Z}_1} \leqslant 86$–$90$ GeV, and also the bounds $m_{\tilde{\tau}_1} \leqslant 76$ GeV, regardless of $m_{\tilde{Z}_1}$. In Fig. 1, in the horizontally hatched region $m_{\tilde{Z}_1} \leqslant 84$ GeV, whereas in the region with vertical hatches, $m_{\tilde{\tau}_1} \leqslant 76$ GeV. Finally, the LEP experiments [22] have a preliminary bound of 91–95 GeV on the mass of the SM Higgs boson. Since, for small values of $\tan\beta$, the lighter Higgs boson h of the GMSB framework is frequently close to the SM Higgs boson, we also show the regions with $m_h \leqslant 95$ GeV (the diagonally hatched area in the lower left corner) in Fig. 1. Furthermore, LEP analyses exclude $m_A \lesssim 83$ GeV when $\tan\beta$ is large. This excludes the thin (diagonally hatched) sliver where $\tan\beta \sim 53$. The reader should appreciate that the various shaded regions that we have shown are not formal experimental limits, but indicate the reach of present experiments within the GMSB framework.

We see from Fig. 1 that current experiments have already probed regions 1 and 2 if $n_5 > 2$. On the other hand, for $n_5 = 1$, we have just these two regions, while $n_5 = 2$, all four regions are still possible. Since experimental signatures within the GMSB framework differ significantly from those in the MSSM and MSUGRA models, it is of interest to reassess the sensitivity of Fermilab Tevatron experiments to signals from sparticle production at the upcoming run II of the Fermilab Tevatron Main Injector (MI) as well as at the proposed luminosity upgrade (dubbed TeV33) where an integrated luminosity ~ 25 fb^{-1} might be accumulated. This is the main purpose of this paper. We had begun this program in an earlier study [6] where we had computed cross sections for various SUSY event topologies for models with $n_5 = 1$ expected at the Fermilab Tevatron: in this case, the NLSP is dominantly the hypercharge gaugino. Here, we first repeat this analysis for somewhat different model parameters, using cuts and acceptances more appropriate to run II. We have also fixed a bug in the program [23] which resulted in an underestimate of the chargino pair production cross section. We also examine cases with larger values of n_5 for which we expect the phenomenology to change qualitatively from our earlier study. Toward this end, we first examine a model line with $n_5 = 2$ with $\tan\beta = 15$ where $\tilde{\tau}_1$ is the NLSP and significantly lighter than other sleptons. Next, we examine a model line with $n_5 = 3$ where all right handed sleptons are roughly degenerate in mass (the co-NLSP scenario), and where $\tilde{e}_1$ ($\tilde{\mu}_1$) dominantly decay via $\tilde{e}_1 \to e\tilde{G}$ ($\tilde{\mu}_1 \to \mu\tilde{G}$). Finally, we examine a non-minimal model where the NLSP is dominantly a Higgsino-like neutralino. This is not because we believe this is any more likely than the MGMSB scenarios previously discussed, but because it leads to qualitatively different experimental signatures. In view of the fact that the underlying mechanism of SUSY breaking, and hence the resulting mass pattern, is unknown, it seems worthwhile to explore implications of unorthodox scenarios, particularly, when they lead to qualitative differences in the phenomenology.

In the next section, we describe the upgrades that we have made to ISAJET to facilitate the simulation of the minimal GMSB framework that we have described, as well as several of its non-minimal extensions. In Sec. III we specify four different model lines and discuss strategies for separating the SUSY signal from SM background for each of these. Our main result is the projection for the reach of experiments at the MI and at TeV33. We end in Sec. IV with a summary of our results together with some general remarks.

II. SIMULATION OF GAUGE MEDIATED SUSY BREAKING SCENARIOS

We use the event generator program ISAJET v 7.40 for simulating SUSY events at the Tevatron. Since ISAJET has been described elsewhere [24], we will only discuss recent improvements that we have made that facilitate the simulation of the MGMSB model specified by the parameter set (1.1), and also, some of its variants. The ''GMSB option'' allows one to use the parameter set (1.1) as an input. ISAJET then computes sparticle masses at the messenger scale M, then evolves these down to the lower scale relevant for phenomenology, and finally calculates the ''MSSM parameters'' that are then used in the evaluation of sparticle cross sections and decay widths. The decays of neutralinos into gravitinos, $\tilde{Z}_i \to \tilde{G}\gamma$, $\tilde{Z}_i \to \tilde{G}Z$, and $\tilde{Z}_i \to \tilde{G}h,H,A$ as well as (approxi-

mately) the Dalitz decay $\tilde{Z}_i \to e^+ e^- \tilde{G}$ are included in ISAJET. The decays $\tilde{l}_1 \to l\tilde{G}$ and $\tilde{\tau}_1 \to \tau\tilde{G}$, as well as the three body decays [25] $\tilde{l}_1 \to \tilde{\tau}_1 \bar{\tau} l$ and $\tilde{l}_1 \to \tilde{\bar{\tau}}_1 \tau l$, which are mediated by a virtual neutralino, have also been included. The widths for corresponding three body decays mediated by virtual chargino exchange are suppressed by the lepton Yukawa coupling, and are also included. These decays can be significant only for smuons, and only when $m_{\tilde{\mu}_1} - m_{\tilde{\tau}_1} \lesssim m_\tau$ so that the neutralino-mediated three body decays of $\tilde{\mu}_1$ are kinematically very suppressed or forbidden. Although for $C_{grav} = 1$, we have not found this to be important, for larger values of C_{grav}, the (long-lived) smuon may dominantly decay via the chargino mediated decay to a stau, and may alter the apparent curvature of the ''smuon track'' in the detector [26].

We have also included in ISAJET the facility to simulate several non-minimal gauge-mediated SUSY breaking models that involve additional parameters. While these will be irrelevant to the analysis performed in our present study, we have chosen to describe this for completeness because it may prove useful to readers studying extensions of the minimal class of models.

The parameter $\mathbb{R}$ allows the user to adjust [27] the ratio between the gaugino and scalar masses by scaling the former by the factor $\mathbb{R}$ which is equal to unity in the minimal GMSB framework.

In GMSB models, additional interactions are needed to generate the dimensional μ and B parameters that are essential from phenomenological considerations. These interactions can split the soft SUSY breaking masses of Higgs and lepton doublets (at the messenger scale) even though these have the same gauge quantum numbers. These additional contributions to the squared masses of Higgs doublets that couple to up and down type fermions, are parametrized [27] by $\delta m^2_{H_u}$ and $\delta m^2_{H_d}$, respectively. These parameters are zero in the minimal model.

If the hypercharge D-term has a non-zero expectation value D_Y in the messenger sector, it will lead to additional contributions to sfermion masses at the messenger scale which may be parametrized [27] as $\delta m^2_{\tilde{f}} = g' Y D_Y$. The value of D_Y (which is zero in the minimal GMSB framework) is constrained as it can lead to an unacceptable pattern of electroweak symmetry.

Finally, allowing incomplete messenger representations [17] can effectively result in different numbers (n_{5_1}, n_{5_2} and n_{5_3}) for each factor of the gauge group. ISAJET allows the user to simulate these non-minimal models using the GMSB2 command.

To model the experimental conditions at the Fermilab Tevatron, we use the toy calorimeter simulation package ISAPLT. We simulate calorimetry covering $-4 \leq \eta \leq 4$ with a cell size given by $\Delta\eta \times \Delta\phi = 0.1 \times 0.087$, and take the hadronic (electromagnetic) calorimeter resolution to be $0.7/\sqrt{E}$ $(0.15/\sqrt{E})$. Jets are defined as hadronic clusters with $E_T > 15$ GeV within a cone of $\Delta R = \sqrt{\Delta\eta^2 + \Delta\phi^2} = 0.7$ with $|\eta_j| \leq 3.5$. Muons and electrons with $E_T > 7$ GeV and $|\eta_l| < 2.5$ are considered to be isolated, if the scalar sum of electromagnetic and hadronic E_T (not including the lepton, of course) in a cone with $\Delta R = 0.4$ about the lepton to be smaller than $max(2\ \text{GeV}, E_T(l)/4)$. Isolated leptons are also required to be separated from one another by $\Delta R \geq 0.3$. We identify photons within $|\eta_\gamma| < 1$ if $E_T > 15$ GeV, and consider them to be isolated if the additional E_T within a cone of $\Delta R = 0.3$ about the photon is less than 4 GeV. Tau leptons are identified as narrow jets with just one or three charged prongs with $p_T > 2$ GeV within 10° of the jet axis and no other charged tracks in a 30° cone about this axis. The invariant mass of these tracks is required to be $\leq m_\tau$ and the net charge of the three prongs required to be ± 1. QCD jets with $E_T = 15 (\geq 50)$ GeV are misidentified as taus [36] with a probability of 0.5% (0.1%) with a linear interpolation in between. Finally, for SVX tagged b-jets, we require a jet (satisfying the above jet criteria) within $|\eta_j| \leq 1$ to contain a B-hadron with $p_T \geq 15$ GeV. The jet is tagged as a b-jet with a probability of 55%. Charm jets (light quark or gluon jets) are mistagged as b-jets with a probability of 5% (0.2%).

III. THE REACH OF TEVATRON UPGRADES FOR VARIOUS MODEL LINES

Within the GMSB framework, sparticle signatures, and hence the reach of experimental facilities, are qualitatively dependent on the nature of the NLSP. Here, we examine the reach of experiments at the Fermilab Tevatron Main Injector as well as that of the proposed TeV33 upgrade for four different model lines [29] where the NLSP is (A) dominantly a hypercharge gaugino, (B) the stau lepton, $\tilde{\tau}_1$, with other sleptons significantly heavier than $\tilde{\tau}_1$, (C) again the stau, but $\tilde{e}_1$ and $\tilde{\mu}_1$ are essentially degenerate with $\tilde{\tau}_1$, and (D) dominantly a Higgsino. We fix the messenger scale $M = 3\Lambda$, $\mu > 0$ and $C_{grav} = 1$ throughout our analysis. We use ISAJET to compute signal cross sections, incorporating cuts and triggers to simulate the experimental conditions at the Fermilab Tevatron together with additional cuts that serve to separate the SUSY signal from SM backgrounds. We project the reach of future Fermilab Tevatron upgrades for each of these scenarios.

A. Model line A: The *B*-ino NLSP scenario

We see from Fig. 1(a) that for $n_5 = 1$, the lightest neutralino is the NLSP as long as $\tan\beta$ is not very large. Since the value of $|\mu|$ computed from radiative breaking of electroweak symmetry is rather large, the NLSP is mainly a B-ino. To realize the B-ino NLSP model line, we fix $\tan\beta = 2.5$ which ensures that sleptons are significantly heavier than $m_{\tilde{Z}_1}$. Sparticles cascade decay to $\tilde{Z}_1$ which then mainly decays via $\tilde{Z}_1 \to \gamma\tilde{G}$. Thus almost all SUSY events contain at least two hard isolated photons.

In Fig. 2(a) we show the mass spectrum of sparticles that might be in the Fermilab Tevatron range versus Λ, which sets the sparticle mass scale, while in frame (b) we show the cross sections for the most important sparticle production mechanisms at the Fermilab Tevatron. We see that chargino

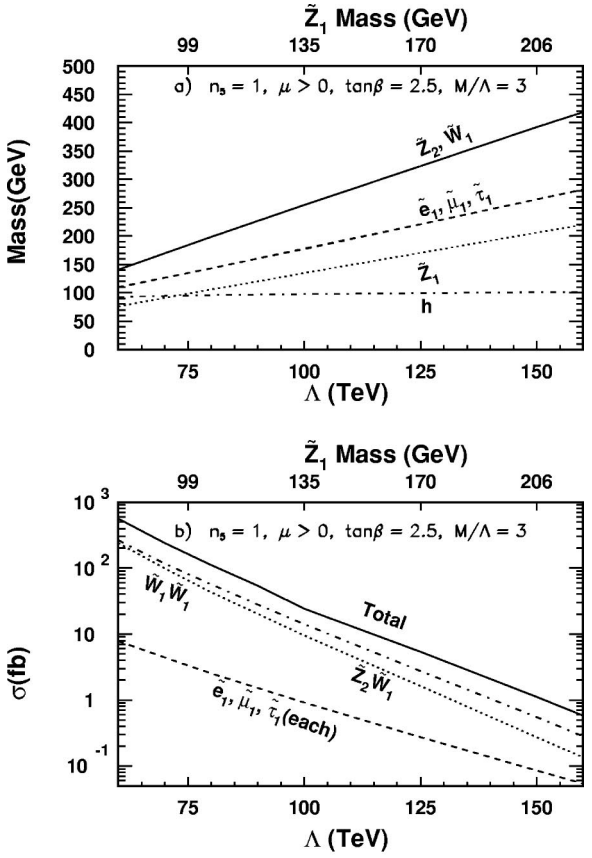

FIG. 2. (a) Relevant sparticle masses and (b) production cross sections for the main sparticle production reactions at a 2 TeV $p\bar{p}$ collider versus the parameter Λ for the *B*-ino NLSP model line A. In frame (b) the dot-dashed line represents the chargino pair production, while the dotted line denotes that for $\tilde{W}_1\tilde{Z}_2$ production. Also shown on the upper axis is the mass of the NLSP.

pair production and $\tilde{W}_1\tilde{Z}_2$ production dominate because squarks and gluinos are beyond the Fermilab Tevatron reach. The production of right-handed slepton pairs is suppressed relative to chargino or neutralino production by over an order of magnitude. Values of Λ smaller than ~ 70 TeV are excluded by the LEP search for $\gamma\gamma + \not{E}_T$ events. For $\Lambda \lesssim 80$ TeV (corresponding to $m_{\tilde{Z}_1} \lesssim 90$–$100$ GeV), the two body decay $\tilde{W}_1 \to W\tilde{Z}_1$ is kinematically suppressed, and the chargino mainly decays via $\tilde{W}_1 \to \tilde{\tau}_1 \nu_\tau$ or $\tilde{W}_1 \to qq\tilde{Z}_1$; for $\Lambda \gtrsim 80$ TeV, the decay $\tilde{W}_1 \to W\tilde{Z}_1$ dominates. The neutralino $\tilde{Z}_2$ dominantly decays via $\tilde{Z}_2 \to \tilde{Z}_1 h$ (for $\Lambda \gtrsim 90$ TeV) when this decay is not kinematically suppressed: otherwise it decays via $\tilde{Z}_2 \to \tilde{l}_1 l$, with roughly equal branching fractions for all three lepton flavors. We thus expect that $\tilde{W}_1\tilde{W}_1$ and $\tilde{Z}_2\tilde{W}_1$ production will mainly lead to jetty events (counting hadronically decaying taus as jets) possibly with additional e and μ plus photons plus $\not{E}_T$.

We use ISAJET to classify the supersymmetric signal events primarily by the number of isolated photons—events with <2 photons arise when one or more of the photons is outside the geometric acceptance, has too low an E_T, or happens to be close to hadrons and thus fails the isolation

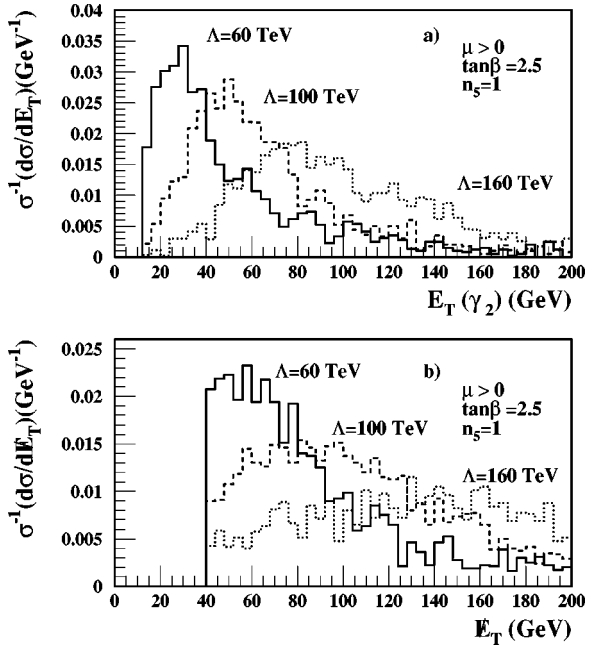

FIG. 3. (a) The transverse energy distribution for the softer photon and (b) the $\not{E}_T$ distribution for the inclusive $\gamma\gamma + \not{E}_T$ for model line A.

requirement. We further separate them into clean and jetty events and then classify them by the number of isolated leptons (e and μ). In addition to the acceptance cuts described in Sec. II, we impose an additional global requirement $\not{E}_T > 40$ GeV, which together with the presence of jets, leptons or photons may also serve as a trigger for these events.

Before proceeding to present results of our computation, we pause to consider SM backgrounds to these events. We expect that the backgrounds are smallest in the two photon channel, which we will mainly focus on for the purpose of assessing the reach. We have not attempted to assess the background because the recent analysis by the DO Collaboration [30], searching for charginos and neutralinos in the GMSB framework, points out that the major portion of the background arises from mismeasurement of QCD jets and for yet higher values of $\not{E}_T$ from misidentification of jets or leptons as photons. In other words, this background is largely instrumental, and hence rather detector-dependent. From Fig. 1 of Ref. [30], we estimate the inclusive $2\gamma + \not{E}_T > 40$ GeV (60 GeV) background level [for $E_T(\gamma_1, \gamma_2) >$ (20 GeV, 12 GeV)] to correspond to $\sim$ 0.9 (0.1) event in their data sample of ~ 100 pb^{-1}. The background from jet mismeasurement, of course, falls steeply with $\not{E}_T$. The inclusive $2\gamma + \not{E}_T$ background is also sensitive to the minimum E_T of the photon.

To assess how changing the photon and $\not{E}_T$ requirements alter the SUSY signal, in Fig. 3 we show the signal distribution of 3(a) $E_T(\gamma_2)$, the transverse energy of the softer photon in two photon events, and 3(b) $\not{E}_T$ in $\gamma\gamma + \not{E}_T$ events that pass our cuts, for three values of Λ. The following is worth noting:

For $\Lambda \simeq 100$ TeV (which we will see is in the range of the Fermilab Tevatron bound), reducing the $E_T(\gamma)$ cut does

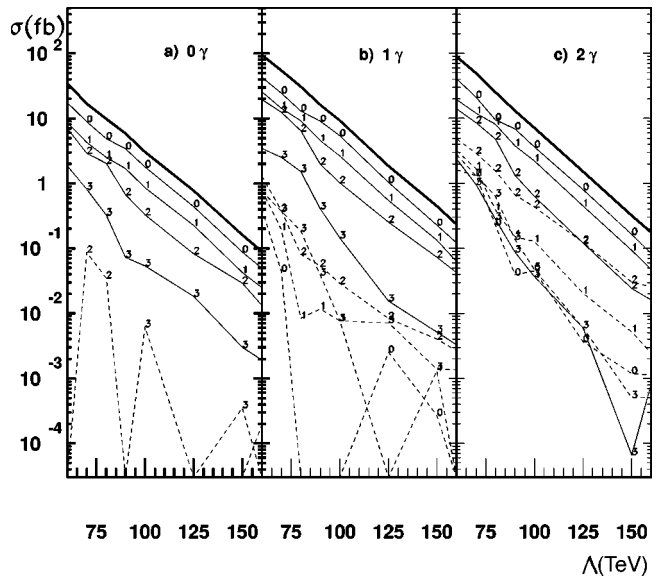

FIG. 4. Topological cross sections for inclusive (a) 0γ, (b) 1γ, and (c) $\gamma\gamma$ plus $\not{E}_T$ signals after the cuts and triggers discussed in the text for model line A. The solid lines denote cross sections for events with at least one jet, while the dashed lines denote cross sections for events with no jets. The numbers on the lines denote the lepton multiplicity. The heavy solid line denotes the total signal cross section after all the cuts.

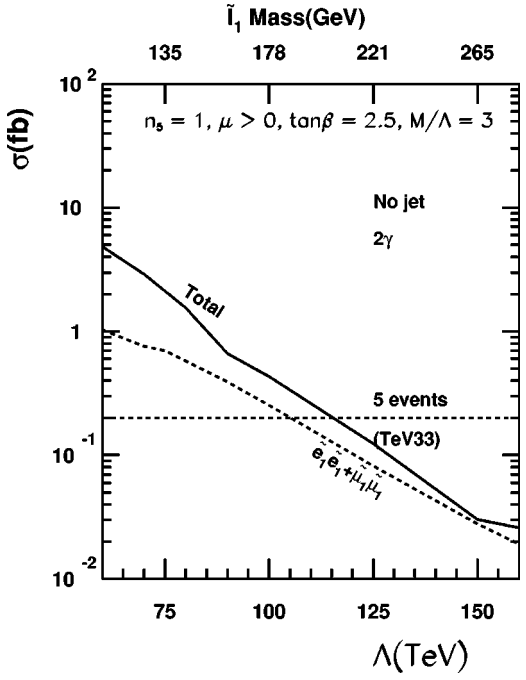

FIG. 5. Signal cross sections for clean $ll\gamma\gamma+\not{E}_T$ events ($l=e,\mu$) from all SUSY sources (solid), and from just $\tilde{e}_1$ or $\tilde{\mu}_1$ pair production (dashed) versus Λ for model line A. The upper scale denotes $m_{\tilde{l}_1}$.

not increase the signal. In fact, it may be possible to further harden this cut to reduce the residual backgrounds. Although we have not shown it here, we have checked that increasing the cut on the *hard* photon to $E_T(\gamma_1)>40$ GeV results in very little loss of signal for $\Lambda>100$ TeV.

In view of our discussion about SM backgrounds, it is clear that requiring $\not{E}_T>60$ GeV greatly reduces the background with modest loss of signal. Indeed, it may be possible to reduce the background to negligible levels by optimizing the cuts on E_T of the photons and on $\not{E}_T$.

The results of our computation of various topological cross sections at a 2 TeV $p\bar{p}$ collider after cuts are shown in Fig. 4 for 4(a) 0 photon, 4(b) one photon, and 4(c) two photon events. In this figure, we have required that $\not{E}_T>60$ GeV. As mentioned, this reduces the cross section by just a small amount, especially for the larger values of Λ in this figure. The solid lines correspond to cross sections for events with at least one jet, while the dashed lines correspond to those for events free of jet activity. The numbers on the lines denote the lepton multiplicity, and are placed at those Λ values that we explicitly scanned. Finally, the heavy solid line represents the sum of all the topologies, i.e., the inclusive SUSY cross section after the cuts. We note the following:

We have comparable signal cross sections in 1γ and 2γ channels. Since the background in the latter is considerably smaller (recall a significant portion of it is from fake photons), the maximum reach is obtained in the 2γ channel.

As anticipated, events with at least one jet dominate clean events, irrespective of the number of photons.

We may obtain a conservative estimate of the reach by assuming an inclusive $2\gamma+\not{E}_T\geqslant 60$ GeV background level of 0.1 event per 100 pb^{-1}, i.e., assuming a background level of 1 fb. This corresponds to a ''5σ reach'' of 3.5 fb (1 fb) for an integrated luminosity of 2 fb^{-1} (25 fb^{-1}) at the Fermilab Tevatron, or $\Lambda\leqslant 110$ TeV (130 TeV) at the Main Injector (TeV33 upgrade). As we have mentioned, it may be possible to further reduce the background by hardening the $E_T(\gamma)$ and $\not{E}_T$ requirements with only modest loss of signal. The background may also be reduced if jet or lepton misidentification as a photon is considerably smaller than in run I [30]. If we optimistically assume that the reach is given by the 5 (10) event level at the Main Injector (TeV33), we would be led to conclude that experiments may probe Λ values as high as 118 TeV (145 TeV) at these facilities. It should be remembered that $\Lambda=118$ TeV corresponds to $m_{\tilde{g}}\sim 950$ GeV, almost equal to what is generally accepted as the qualitative upper limit from fine tuning arguments.

We see from Fig. 2(b) that the $\tilde{l}_1\tilde{l}_1$ production cross section exceeds 1 fb for $\Lambda\leqslant 100$ TeV. Since slepton production can lead to spectacular $ll\gamma\gamma+\not{E}_T$ events of the type observed by the Collider Detector at Fermilab (CDF) Collaboration [31], it appears reasonable to ask whether signal from slepton pair production might be observable at TeV33, and further, whether it can be separated from a similar signal from chargino pair production when each $\tilde{W}_1\to l\nu\tilde{Z}_1\to l\nu\tilde{G}\gamma$ [32]. The SM *physics* backgrounds come from $WW\gamma\gamma$ production which for $E_{T\gamma}\geqslant 10$ GeV has a production cross section [31] of 0.15 ± 0.05 fb, so that ~ 0.1 such event is expected in a data sample of 25 fb^{-1}. The background from $t\bar{t}$ production is estimated to be even smaller. In Fig. 5 we show the total cross section for clean $ll\gamma\gamma+\not{E}_T$ events after cuts

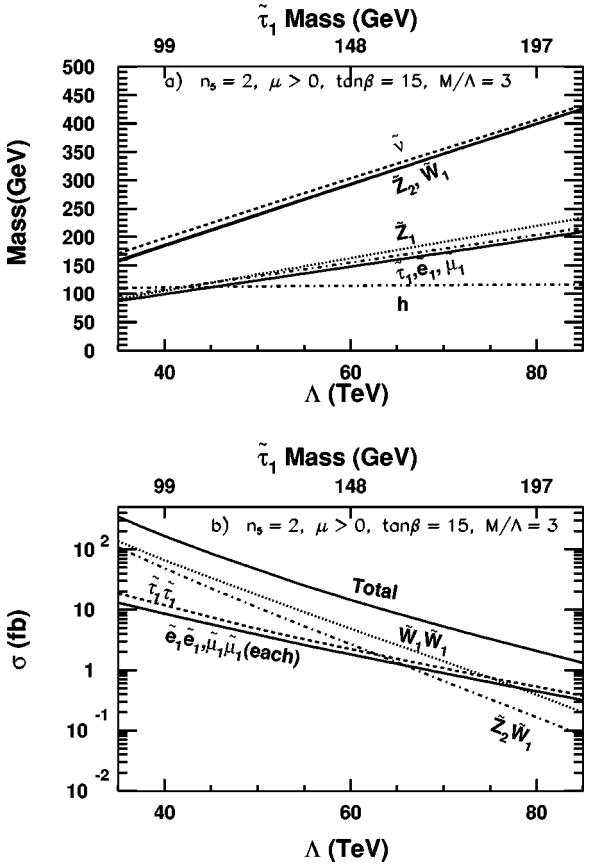

FIG. 6. The same as Fig. 2, but for the stau NLSP model line B. In frame (a) the solid line denotes the mass of $\tilde{\tau}_1$, while the dot-dashed line denotes the mass of the lighter selectron or smuon which are very nearly degenerate.

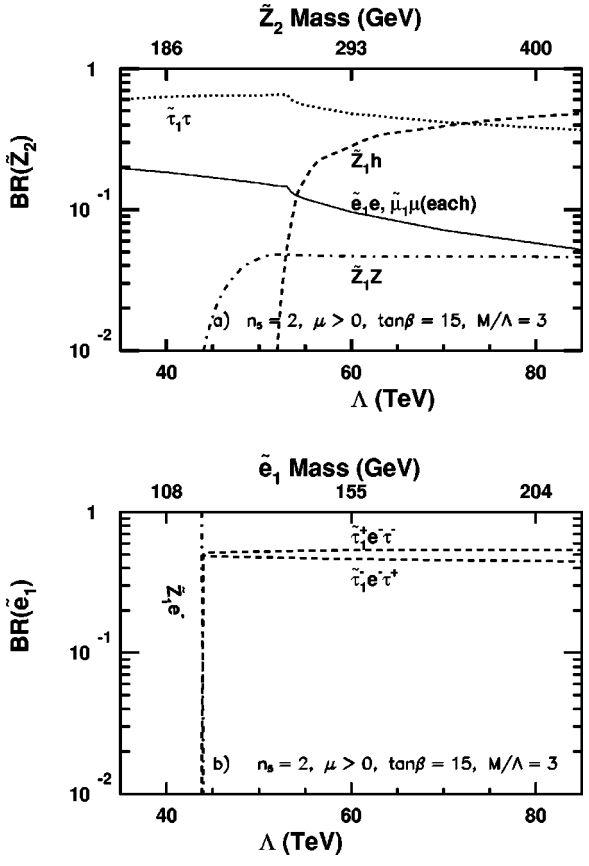

FIG. 7. The branching ratios for various decays of (a) $\tilde{Z}_2$, and (b) $\tilde{l}_1$ for model line B. The upper scale shows the mass of the parent sparticle. The relevant decay patterns of other sparticles are described in the text.

(solid) and the corresponding cross section from just $\tilde{e}_1$ and $\tilde{\mu}_1$ pair production (dashed). We see that for $\Lambda \lesssim 115$ TeV (corresponding to $m_{\tilde{l}_1} \sim 200$ GeV), five or more signal events should be present at TeV33, with about 60% of these having their origin in direct production of sleptons. Slepton pair production alone yields five events for $m_{\tilde{l}_1} \lesssim 180$ GeV. If instrumental backgrounds from jets faking an electron or photon turn out to be negligible, direct detection of sleptons as heavy as 180 GeV may be possible at TeV33 [33] for model line A.

B. Model line B: The stau NLSP scenario

From Fig. 1, we see that we can obtain $\tilde{\tau}_1$ as the NLSP for a wide range of GMSB parameters. Here, we choose $n_5 = 2$, and take $\tan\beta = 15$ to make $\tilde{e}_1$ and $\tilde{\mu}_1$ somewhat heavier than $\tilde{\tau}_1$, with other parameters as before. In Fig. 6 we show (a) relevant sparticle masses and (b) cross sections for the main sparticle production mechanisms versus Λ. For $\Lambda \gtrsim 30$ TeV, $m_{\tilde{\tau}_1} \leq m_{\tilde{Z}_1}$ but for $\Lambda \lesssim 32$ TeV, $\tilde{Z}_1 \to \tau\tilde{\tau}_1$ is kinematically forbidden, and $\tilde{Z}_1$ would decay via the four body decay $\tilde{Z}_1 \to \nu_\tau \tilde{\tau}_1 W^*$ (which is not yet included in ISAJET) or via its photon mode considered above. In our study, we only consider $\Lambda \geq 35$ TeV, the region safe from LEP constraints. Gluinos and squarks are then too heavy to be produced at the Fermilab Tevatron, and sparticle production is dominated by chargino, neutralino and, to a lesser extent, slepton pair production.

The two body decay $\tilde{W}_1 \to \tilde{\tau}_1 \nu$ is always accessible, while the decay $\tilde{W}_1 \to W\tilde{Z}_1$ becomes significant only for $\Lambda \gtrsim 45$ TeV ($m_{\tilde{W}_1} \gtrsim 210$ GeV). The branching fraction for $\tilde{Z}_2$ decays are shown in Fig. 7(a). We see that $\tilde{Z}_2$ decays via $\tilde{\tau}_1\tau$ with a branching fraction that exceeds 0.5 if $m_{\tilde{Z}_2} \lesssim 300$ GeV, and further that branching fractions for $\tilde{Z}_2 \to \tilde{l}_1 l$ ($l = e, \mu$) are not negligible. For the value of $\tan\beta$ in this figure, the decay $\tilde{Z}_2 \to \tilde{Z}_1 h$ is only important for relatively large values of Λ. The lightest neutralino $\tilde{Z}_1$ mainly decays via $\tilde{Z}_1 \to \tilde{\tau}_1 \tau$, though for large enough values of Λ, its decay to sleptons of other families may also be significant. The decay pattern of the lighter selectron and smuon are illustrated in Fig. 7(b). For small values of Λ (region 2 of Fig. 1), the decay $\tilde{l}_1 \to l\tilde{Z}_1$ is kinematically allowed and dominates. For larger values of Λ (region 4 of Fig. 1), where this channel is closed, the neutralino is virtual and $\tilde{l}_1^- \to \tilde{\tau}_1^+ l^- \tau^-$ or $\tilde{l}_1^- \to \tilde{\tau}_1^- l^- \tau^+$. These decays dominate the de-

TABLE I. SM background cross sections in fb for various clean multilepton topologies from W, $Z \to \tau\tau$, VV $(V=W,Z)$ and $t\bar{t}$ production at a 2 TeV $p\bar{p}$ collider, together with signal cross sections for $\Lambda = 40$ TeV and $\Lambda = 50$ TeV for model line B described in the text. For each event topology, the first number denotes the cross section after the basic acceptance cuts and trigger requirements along with the Z veto and the $\Delta\phi$ cut discussed in the text. The second number is after the additional cut, $p_{T vis}(\tau_1) \geqslant 40$ GeV, for events at least one identified τ. The entries labelled Total* are the sum of all the cross sections except those in the $1\tau 1l$ channel. The last two rows provide a measure of the statistical significance of the signal.

Topology	W	$Z \to \tau\tau$	VV	$t\bar{t}$	$\Lambda = 40$ TeV	$\Lambda = 50$ TeV
$C3l$	0	0	0.39	0	0.68	0.24
	0	0	0.39	0	0.68	0.24
$C1\tau 1l$	1045	4.2	36	0.044	8.6	1.96
	43	2.0	10.8	0	5.3	1.27
$C1\tau 2l$	0	0.57	1.4	0	3.3	0.93
	0	0.045	0.43	0	1.9	0.59
$C1\tau 3l$	0	0	0	0	0.31	0.16
	0	0	0	0	0.21	0.10
$C2\tau 1l$	0	1.5	1.2	0	4.1	1.2
	0	0.57	0.79	0	3.3	1.02
$C2\tau 2l$	0	0	0	0	0.36	0.23
	0	0	0	0	0.33	0.22
Total*	0	2.1	2.99	0	8.75	2.76
	0	0.62	1.61	0	6.42	2.17
$\sigma(\text{sgn})/\sqrt{\sigma(\text{back})}$ $(\text{fb}^{1/2})$					3.87	1.22
					4.30	1.45

cay $\tilde{l}_1 \to l\tilde{G}$. The upshot of these decay patterns is that SUSY events may contain several tau leptons from sparticle cascade decays. At the very least, each event will contain a pair of τs (in addition to other leptons, jets and $\not{E}_T$) from $\tilde{\tau}_1$ produced at the end of the decay cascade. It is worthwhile to note that the two τs could easily have the same sign of electric charge.

The observability of SUSY realized as in this scenario thus depends on the capability of experiments to identify hadronically decaying tau leptons, and further, to distinguish these from QCD jets. Following the same logic as in the $n_5 = 1$ case above, we now classify SUSY events by the number of identified taus, and further separate them into jetty and clean event topologies labeled by the number of isolated leptons (e and μ). It should be remembered that the efficiency for identifying taus is expected to be smaller than for identifying photons—first, the tau has to decay hadronically, and then the hadronic decay products have to form a jet.

In our analysis, in addition to the basic acceptance cuts discussed in Sec. II, we require $\not{E}_T \geqslant 30$ GeV together with at least one of the following which serve as a trigger for the events:

one lepton with $p_T(l) \geqslant 20$ GeV,
two leptons each with $p_T(l) \geqslant 10$ GeV,
$\not{E}_T \geqslant 35$ GeV.

In addition, we also impose the additional requirements:

a veto on opposite sign, same flavor dilepton events with $M_Z - 10$ GeV $\leqslant m(l\bar{l}) \leqslant M_Z + 10$ GeV to remove backgrounds from WZ and ZZ and high p_T Z production, and

for dilepton events, require $\Delta\phi(l\bar{l'}) \leqslant 150°$ $(l,l' = e,\mu,\tau)$ to remove backgrounds from $Z \to \tau\bar{\tau}$ events.

The dominant physics sources of SM backgrounds to n-jet + m-leptons + $\not{E}_T$ events, possibly containing additional taus, are W, γ^* or Z + jet production, $t\bar{t}$ production, and vector boson pair production. Instrumental backgrounds that we have attempted to estimate are $\not{E}_T$ from mismeasurement of jet energy and mis-identification of QCD jets as taus.

We have checked that even after these cuts and triggers, SM backgrounds from W production swamp the signal in channels with no leptons or just one identified lepton (e, μ, or τ). The former is the canonical $\not{E}_T$ signal, which after optimizing cuts, may be observable at run 2 if gluinos are lighter than ~ 400 GeV. We do not expect that this signal from gluino and squark production will be detectable, since even for $\Lambda = 35$ TeV, $m_{\tilde{g}} = 578$ GeV with squarks somewhat heavier. For this reason, and because there are large single lepton backgrounds from W production, we focus on signals with two or more leptons in our study. Also, because the presence of τ's is the hallmark of this scenario, we mostly concentrate on leptonic events with at least one identified τ.

We begin by considering the signal and background cross sections for clean events. These are shown in Table I. Events are classified first by the number of identified taus, and then by the lepton multiplicity; the C in the topology column denotes ''clean'' events. For each topology, the first row of numbers denotes the cross sections after the basic acceptance cuts and trigger requirements along with the Z veto and the

TABLE II. SM background cross sections in fb for various jetty multilepton topologies from W, $Z \to \tau\tau$, VV $(V=W,Z)$ and $t\bar{t}$ production at a 2 TeV $p\bar{p}$ collider, together with signal cross sections for $\Lambda = 40$ TeV and $\Lambda = 50$ TeV for model line B described in the text. The cross sections are with all the cuts including the p_{Tvis} cut on the hardest τ.

Topology	W	$Z \to \tau\tau$	VV	$t\bar{t}$	$\Lambda = 40$ TeV	$\Lambda = 50$ TeV
$J3l$	0	0.019	0.28	0.3	1.06	0.35
$J1\tau 2l$	0	0.19	0.29	1.2	1.92	0.79
$J2\tau 1l$	0.11	0.79	0.41	0.8	2.25	1.18
$J2\tau 2l$	0	0	0	0	0.31	0.22
Total	0.11	1.0	0.98	2.3	5.53	2.54
$\sigma(\text{sgn})/\sqrt{\sigma(\text{back})}$ $(\text{fb}^{1/2})$					2.64	1.21

$\Delta\phi$ cut discussed above. We see that there is still a substantial background in several of the multilepton channels. This background can be strongly suppressed, with modest loss of signal by imposing an additional requirement,

$p_{Tvis}(\tau_1) \geq 40$ GeV, on the visible energy of the hardest tau in events with at least one identified tau. In the background, the τs typically come from vector boson decays, while in the signal, a substantial fraction of these come from the direct decays of charginos and neutralinos that are substantially heavier than M_Z [remember even $m_{\tilde{Z}_1} = 103$ (132) GeV for $\Lambda = 40$ (50) TeV]: thus signal taus pass this cut more easily. A few points about this table are worth mentioning.

(1) The signal cross sections in each channel are at most a few fb, and with an integrated luminosity of 2 fb^{-1}, the individual signals are below the 5σ level even for $\Lambda = 40$ TeV. For the integrated luminosity expected in run II of the MI, we will be forced to add the signal in various channels and see if this inclusive signal is observable.

(2) The sum of the signal in all the channels in Table I, except the $1\tau 1l$ channel which has a very large background, is shown in the next two rows both with and without the p_T cut on the τ, while in the last two rows we list $\sigma(\text{sgn})/\sqrt{\sigma(\text{back})}$. We see that a somewhat better significance is obtained after the $p_{Tvis}(\tau_1) \geq 40$ GeV cut.

(3) We see that the inclusive SUSY signal in the clean channels for the $\Lambda = 40$ TeV case should be detectable with the run II integrated luminosity, whereas for the $\Lambda = 50$ TeV case, an integrated luminosity of 12 fb^{-1} is needed for a 5σ signal.

(4) We caution the reader that about 25–30% of the τ background comes from mis-tagging QCD jets as taus (except, of course, for the W backgrounds and the backgrounds in the $C2\tau l$ channels which are almost exclusively from these fake taus). Thus our estimate of the background level is somewhat sensitive to the τ faking algorithm we have used. The signal, on the other hand, almost always contains only real τs, so that improving the discrimination between τ and QCD jets will lead to an increase in the projected reach of these experiments.

(5) In some channels the background is completely dominated by fake taus. For instance, after the $p_{Tvis}(\tau)$ cut, the $C1\tau 1l$ background from W sources of just *real taus* is only 1.9 fb, while the signal and other backgrounds remain essentially unaltered from the cross sections in Table I. Thus if fake τ backgrounds can be greatly reduced, it may be possible to see a signal via other channels.

Next, we turn to jetty signals for model line B. Cross sections for selected signal topologies together with SM backgrounds *after* the $p_T(\tau_1) \geq 40$ GeV cut are shown in Table II. The other topologies appear to suffer from large SM backgrounds and we have not included them here.

The following features are worth noting:

(1) We see that model line B results in smaller cross sections in jetty channels. This should not be surprising, since electroweak production of charginos, neutralinos, and sleptons are the dominant SUSY processes, and because staus are light, branching fractions for hadronic decays of $\tilde{W}_1$ and $\tilde{Z}_{1,2}$ tend to be suppressed.

(2) We see from Table II that with the present set of cuts, not only is the signal below the level of observability in any one of the channels, but also that the inclusive signal is not expected to be observable at the MI even for the $\Lambda = 40$ TeV case. With an integrated luminosity of 25 fb^{-1}, the signal for the $\Lambda = 50$ TeV case is observable at the 6σ level.

(3) As for the clean lepton case, a significant portion of the background comes from QCD jets faking a tau. The fraction of events with a fake tau varies from channel to channel, but for the $2\tau 1l$ channel in Table II, almost 60% of the background (in contrast to essentially none of the signal) involves at least one fake τ.

(4) A major background to the jetty signal comes from $t\bar{t}$ production. To see if we could enhance the signal relative to this background, we tried to impose additional cuts to reduce selectively the top background. Since top events are expected to contain hard jets, we first tried to require $E_T(j) \leq 50$ GeV. We also, independently, tried vetoing events where the invariant mass of all jets exceeded 70 GeV. While both attempts lead to an improvement of the signal to background ratio, the statistical significance of the signal is not improved (and is even degraded) by these additional cuts. We do not present details about this for the sake of brevity. It may be possible to reduce the top background by vetoing events with tagged b-jets, but we have not attempted to do so here.

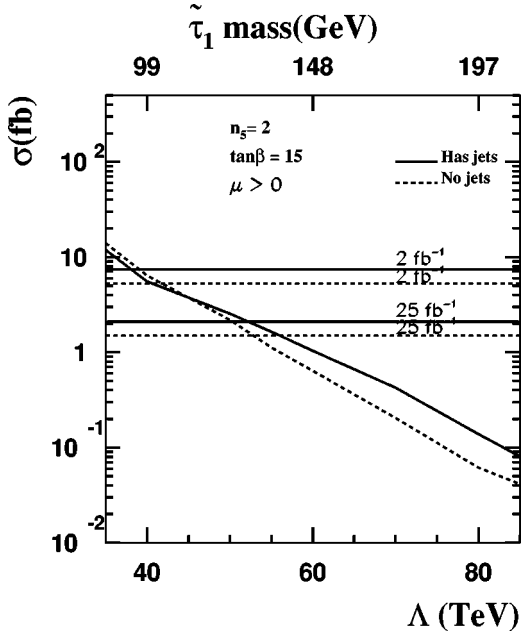

FIG. 8. Signal cross sections after all cuts versus Λ for the total signal in the clean (dashed line) and jetty (solid line) channels shown in Table I and Table II, respectively, for model line B. The corresponding horizontal lines denote the minimum cross section for a 5σ signal, both at the MI and at TeV33.

For model line B, it appears that experiments at the MI should be able to probe Λ values up to just beyond 40 TeV in the inclusive clean multilepton channels. It appears, however, that it will be essential to sum up several channels to obtain a signal at the 5σ level. Confirmatory signals in inclusive jetty channels may be observable at the 3.7σ level. Of course, for an integrated luminosity of 25 fb^{-1}, it may be possible to probe $\Lambda=50$ TeV even in the unfavored jetty channels, and somewhat beyond in the clean channels. The situation is summarized in Fig. 8 where we show the signal cross sections summed over the selected channels for events without jets (dashed) and for events with jets (solid). The horizontal lines denote the minimum cross section needed for the signal to be observable at the 5σ level, for the two assumptions about the integrated luminosity. We note that, in some channels, a susbtantial fraction of background events come from QCD jets faking a tau—our assessment of the run II reach is thus sensitive to our modelling of this jet mis-tag rate. By the same token, if this rate can be reduced, the reach may be somewhat increased. Finally, we remark that even though it appears that the range of parameters that is accessible to experiments at the MI is very limited ($\Lambda \leqslant 42$ TeV), these parameters correspond to charginos as heavy as 192 GeV and gluinos and squarks around 700 GeV.

C. Model line C: The co-NLSP scenario

This scenario can simply be obtained by choosing parameters in regions 3 of Fig. 1, so that $\tilde{e}_1$, $\tilde{\mu}_1$ and $\tilde{\tau}_1$ are all approximately degenerate, and $\tilde{e}_1$ and $\tilde{\mu}_1$ cannot decay to $\tilde{\tau}_1$. Here, we choose $n_5=3$ and $\tan\beta=3$ with other parameters as before. In Fig. 9 we show 9(a) relevant sparticle masses,

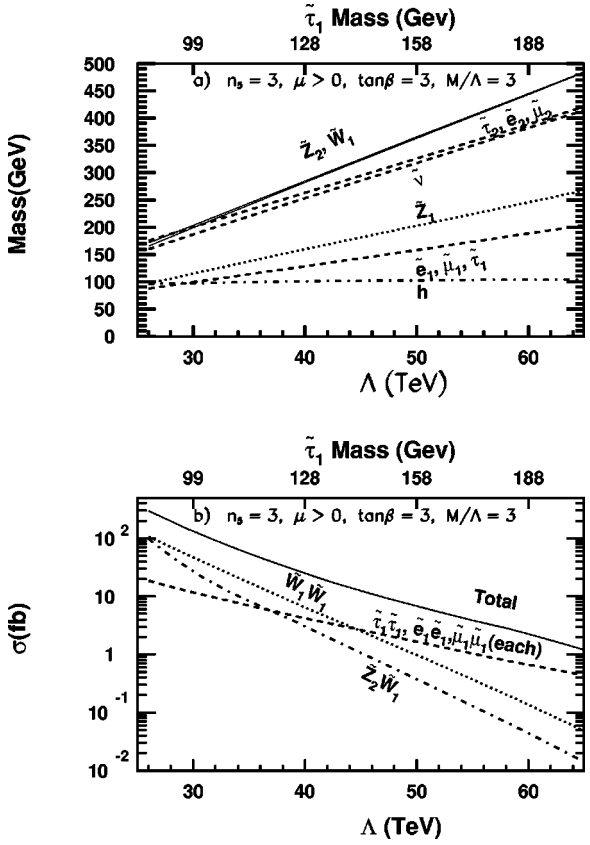

FIG. 9. The same as Fig. 2, but for the co-NLSP model line C.

and 9(b) cross sections for the main sparticle production mechanisms at the Fermilab Tevatron versus Λ. Aside from the fact that lighter sleptons of all three flavors have essentially the same mass, the main difference from the earlier model lines that we have studied is that, while charginos and neutralinos dominate for lower values of Λ, slepton pair production is the dominant production mechanism for $\Lambda \gtrsim 40$ TeV (corresponding to $m_{\tilde{l}} \gtrsim 125$ GeV).

In Fig. 10 we show the branching fractions for 10(a) chargino, and 10(b) neutralino decays versus Λ. For small Λ in frame 10(a), charginos dominantly decay via $\tilde{W}_1 \to \tilde{\tau}_1 \nu_\tau$, since the corresponding decays to smuons and selectrons are suppressed by the lepton Yukawa coupling. As Λ increases, decays to sneutrinos and the heavier (dominantly left-handed) sleptons become accessible. Since these occur via (essentially unsuppressed) gauge interactions, these rapidly dominate the decay to $\tilde{\tau}_1$. The decay $\tilde{W}_1 \to \tilde{Z}_1 W$ also becomes significant for $m_{\tilde{W}_1} \gtrsim 200$ GeV. Turning to $\tilde{Z}_2$ decays shown in frame 10(b), we see that these dominantly decay to sleptons with branching fractions more or less independent of the lepton flavor. Again, since $\tilde{Z}_2$ is dominantly an $SU(2)$ gaugino, decays to the heavier (dominantly left-handed) sleptons and sneutrinos dominate when these are kinematically unsuppressed. The branching fraction for the decay $\tilde{Z}_2 \to \tilde{Z}_1 h$ is also significant. From the plot of sparticle masses in Fig. 9a, we see that the heavier charged sleptons and sneutrinos decay via $\tilde{f}_2 \to f \tilde{Z}_1$, while $\tilde{f}_1 \to f \tilde{G}$ $(f = l, \nu)$.

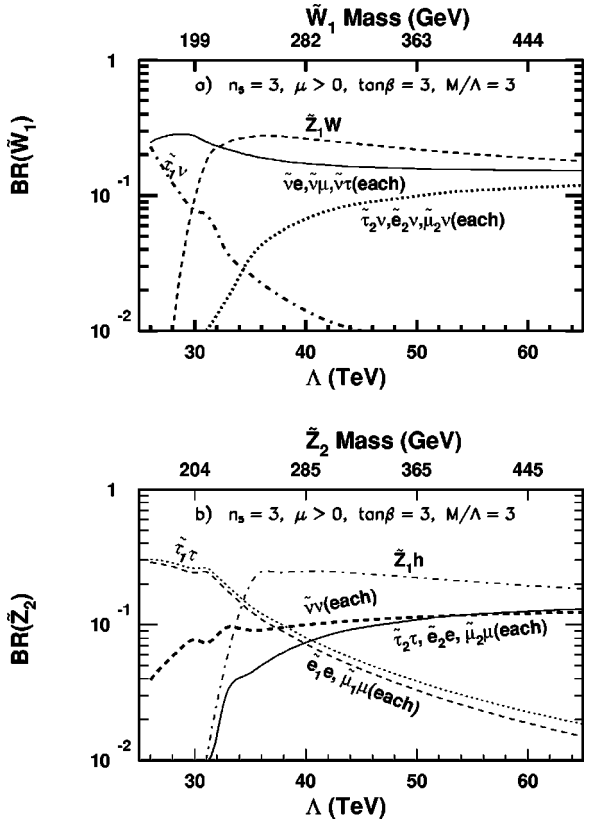

FIG. 10. Branching ratios for decays of (a) $\tilde{W}_1$ and (b) $\tilde{Z}_2$ for model line C. Decay patterns of other sparticles are discussed in the text.

The lightest neutralino decays via $\tilde{Z}_1 \to \tilde{l}_1 l$ with branching fractions essentially independent of the lepton flavor.

The bottom line of these decay patterns is that even though $\tilde{\tau}_1$ is strictly speaking the NLSP, we expect a large multiplicity of isolated leptons (e and μ) from sparticle production at colliders. This is because all flavors of sleptons are roughly equally produced in SUSY cascade decays, and decays of $\tilde{e}_1$ and $\tilde{\mu}_1$ do not involve a stau at an intermediate stage. This is illustrated in Fig. 11 for $\Lambda = 30$ TeV and $\Lambda = 40$ TeV, where we show the multiplicity distributions for both $n_e + n_\mu$ and $n_e + n_\mu + n_\tau$, for events satisfying the basic acceptance cuts (see Sec. II) and trigger conditions, but not the additional requirements described in Sec. III B. We see that while the lepton multiplicity is largest for two leptons (due to production of l_R pairs), a very sizeable fraction of signal events have both $n_e + n_\mu$ and $n_e + n_\mu + n_\tau \geq 4$ for which backgrounds from SM sources, shown in Table III, are very small. Here, for the $n_e + n_\mu + n_\tau \geq 4$ background sample, we found that all the background events that passed the cuts automatically satisfied $n_e + n_\mu \geq 2$. We also impose this requirement, which should facilitate triggering on these events even without a τ trigger, on the signal [34].

In our simulation, we found that the background from W and Z plus jet production, as well as $t\bar{t}$ production are negligible. We see that the 4-lepton background is an order of magnitude smaller than the corresponding $3l$ backgrounds in Tables I and II (even though the cuts there are more stringent

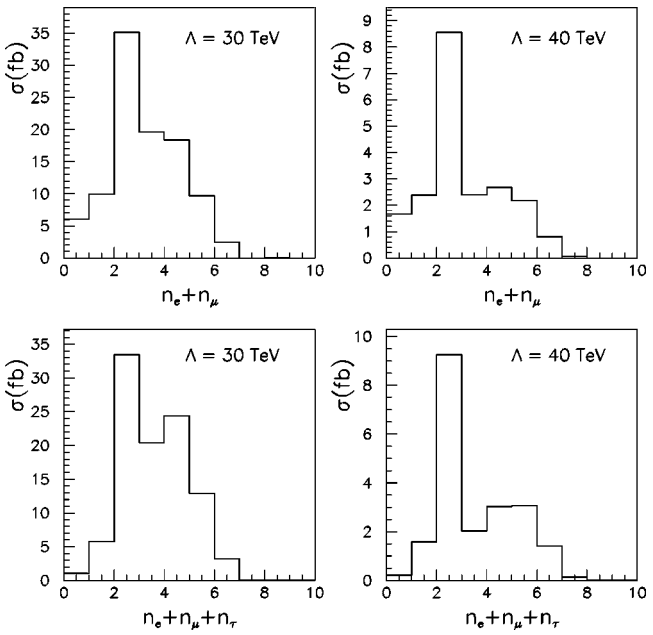

FIG. 11. Lepton multiplicity distributions for SUSY events after all cuts with $\Lambda = 30$ TeV, and $\Lambda = 40$ TeV for model line C. We show distributions of both $n_e + n_\mu$ and $n_e + n_\mu + n_\tau$, where n_τ is the multiplicity of tagged τ leptons in the event.

than in Table III). In contrast, for the signal, we see from Fig. 11 that the rate for $3l$ events is much smaller than that for $\geq 4l$ events. Thus the $\geq 4l$ channel offers the best hope for detection of the SUSY signal for model line C.

The SUSY reach for the co-NLSP model line is illustrated in Fig. 12 where we show the signal cross section versus Λ for inclusive events with $n_e + n_\mu \geq 4$ (dashed) and $n_e + n_\mu + n_\tau \geq 4$ (solid) where we require, in addition, $n_e + n_\mu \geq 2$. Here we have summed the cross section for events with and without jets as this offers the greatest reach. The corresponding horizontal lines denote the levels where the signal will be just detectable at the ''5σ level'' (with a minimum of at least five events) at the MI and at the proposed TeV33 upgrade. We observe the following:

With an integrated luminosity of 2 fb^{-1}, the signal is rate-limited in the $n_e + n_\mu \geq 4$ channel, and experiments at

TABLE III. SM background cross sections in fb for clean and jetty events with ≥ 4 leptons from VV ($V = W, Z$) production at a 2 TeV $p\bar{p}$ collider, after the basic cuts and triggers described in the text. At least 2 leptons are required to be e or μ. Backgrounds from Z, W and $t\bar{t}$ production are negligible. Also shown are corresponding signal cross sections for $\Lambda = 30$ TeV and $\Lambda = 40$ TeV for model line C described in the text. As before, the C (J) refers to clean and jetty events.

Topology	VV	$\Lambda = 30$ TeV	$\Lambda = 40$ TeV
$C: n_e + n_\mu \geq 4$	0.09	14.0	2.3
$C: n_e + n_\mu + n_\tau \geq 4$	0.30	19.0	3.0
$J: n_e + n_\mu \geq 4$	0	16.5	3.4
$J: n_e + n_\mu + n_\tau \geq 4$	0.33	21.2	4.5

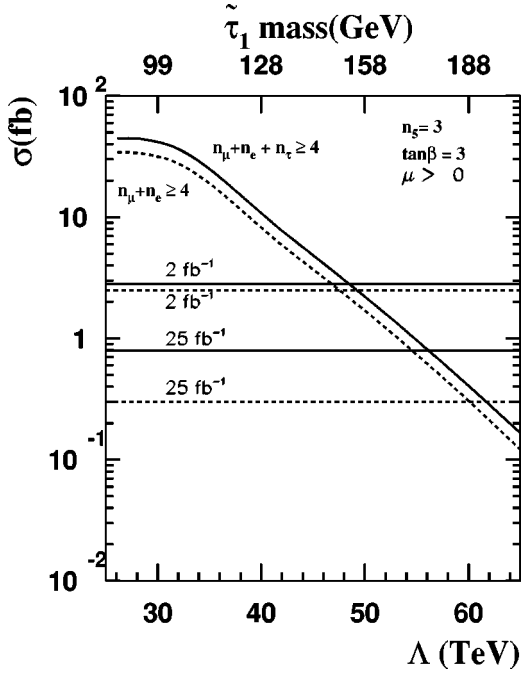

FIG. 12. Signal cross sections after all cuts for SUSY events with $n_e+n_\mu+n_\tau \geq 4$ (solid) and $n_e+n_\mu \geq 4$ (dashed) for model line C. The corresponding horizontal lines denote the minimum cross section for a 5σ signal (with a minimum of five signal events) at the MI and at TeV33.

the MI should be able to probe Λ out to about 45 TeV (corresponding to charginos heavier than 300 GeV) if we require a minimum signal level of five events. Including taus increases the signal, but also increases the background so that the reach is only marginally improved. Since this background largely comes from tau mis-identification, it should be kept in mind that our projection for the reach via the $n_e+n_\mu+n_\tau \geq 4$ channel is somewhat dependent on our simulation of this.

For an integrated luminosity of 25 fb^{-1}, we see that the projected increase in the background in the channel that includes taus actually leads to a *reduction* of the reach, and the greatest reach is obtained via events with $n_e+n_\mu \geq 4$ leptons for which the background is very small. In our assessment of this reach, we have assumed that backgrounds from hadrons or jets mis-identified es and μs are negligible. The reach of TeV33 experiments should then extend to $\Lambda \lesssim 55$ TeV which corresponds to $m_{\tilde{W}_1}(m_{\tilde{g}}) \lesssim 400(1200)$ GeV.

Although we have not shown this here, we have checked that the same sign dilepton channel does not yield a better reach than the $4l$ channel just discussed. Typically, cross sections in this channel are about 10–25% of the total dilepton cross section in Fig. 11, whereas SM backgrounds (with just the basic cuts and triggers) are in the several fb range.

D. Model line D: The Higgsino NLSP scenario

Within the GMSB framework described above, the value of $|\mu|$ that we obtain tends to be considerably larger than M_1 and M_2, so that the lightest neutralino is dominantly a gaugino (more specifically a bino, since $M_1 \simeq \frac{1}{2}M_2$). This is indeed the case for the three model lines examined above. Motivated by the fact that the phenomenology is very sensitive to the nature of the NLSP, we have examined a non-minimal scenario where we alter the ratio of $|\mu|/M_1$ by hand from its model value, and fix a small value of $|\mu|$ so that the NLSP is mainly Higgsino-like. We do not attempt to construct a theoretical framework which realizes such a scenario, but only mention that the additional interactions needed to generate μ and also the B-parameter in this framework could conceivably alter the relation between μ and the gaugino masses. With this in mind, we use ISAJET to simulate a light Higgsino scenario where we take $n_5=2$, $\tan\beta=3$, $M/\Lambda=3$, $C_{grav}=1$, but fix $\mu=-\frac{3}{4}M_1$ rather than the value obtained from radiative electroweak symmetry breaking. In practice, we do so by using the weak scale parameters obtained using the GMSB model in ISAJET as input parameters for the MSSM model, except that we use $\mu=-\frac{3}{4}M_1$ at this juncture. For this ''small μ'' scenario, we expect that the two lightest neutralino and the lighter chargino will be Higgsino-like and close in mass, while the heavier charginos and neutralinos will be gaugino-like. The resulting spectrum is shown in Fig. 13(a). Indeed we see that $\tilde{Z}_1$ is the NLSP over the entire parameter range shown, and that $\tilde{Z}_2$ and $\tilde{W}_1$ are generally only 20–30 GeV heavier. As a result, the fermions from $\tilde{W}_1$ and $\tilde{Z}_2$ decays to $\tilde{Z}_1$ will be rather soft. Slepton masses are essentially family-independent because $\tan\beta$ is small. The lighter Higgs boson mass is just above 100 GeV, independent of Λ.

Sparticle production at the Tevatron is dominated by the production of these Higgsino-like charginos and neutralinos as can be seen in Fig. 13(b). An important difference between this case and chargino and neutralino production in the model lines examined above is that $\tilde{W}_1\tilde{Z}_1$ and $\tilde{Z}_1\tilde{Z}_2$ production is also substantial. For a fixed chargino mass, however, the sparticle production cross section is somewhat smaller for model line C than it is for the other model lines.

We have already noted that fermions from the decays $\tilde{W}_1 \to f\bar{f}'\tilde{Z}_1$ and $\tilde{Z}_2 \to f\bar{f}\tilde{Z}_1$ are generally expected to be soft so that signatures for $\tilde{Z}_i\tilde{Z}_j$ or $\tilde{Z}_i\tilde{W}_j$ production will closely resemble those for $\tilde{Z}_1\tilde{Z}_1$ production. In other words, sparticle signatures in such a scenario will be mainly determined by the $\tilde{Z}_1$ decay pattern shown in Fig. 14. For small values of Λ, $\tilde{Z}_1 \to \tilde{G}\gamma$. As Λ increases, the decays $\tilde{Z}_1 \to \tilde{G}Z$ and $\tilde{Z}_1 \to \tilde{G}h$ become kinematically accessible, and the branching fraction for the photon decay becomes unimportant, while the decay to the Higgs boson becomes dominant. This is in sharp contrast to the gaugino NLSP case where the decay to the Higgs scalar is strongly suppressed.

For small values of Λ (where $\tilde{Z}_1$ mainly decays to via $\tilde{Z}_1 \to \tilde{G}\gamma$), the strategy for extracting the SUSY signal is as for model line A; i.e., to look for inclusive $2\gamma+\not{E}_T$ events. If we adopt the conservative background level of 1 fb as in this study, a ''5σ'' reach is obtained at the MI (TeV33) provided the signal cross section exceeds 3.5 fb (1 fb). These levels are shown as the horizontal dashed lines in Fig. 15, while the corresponding signal is shown by the curve labeled $\sigma(\gamma\gamma)$.

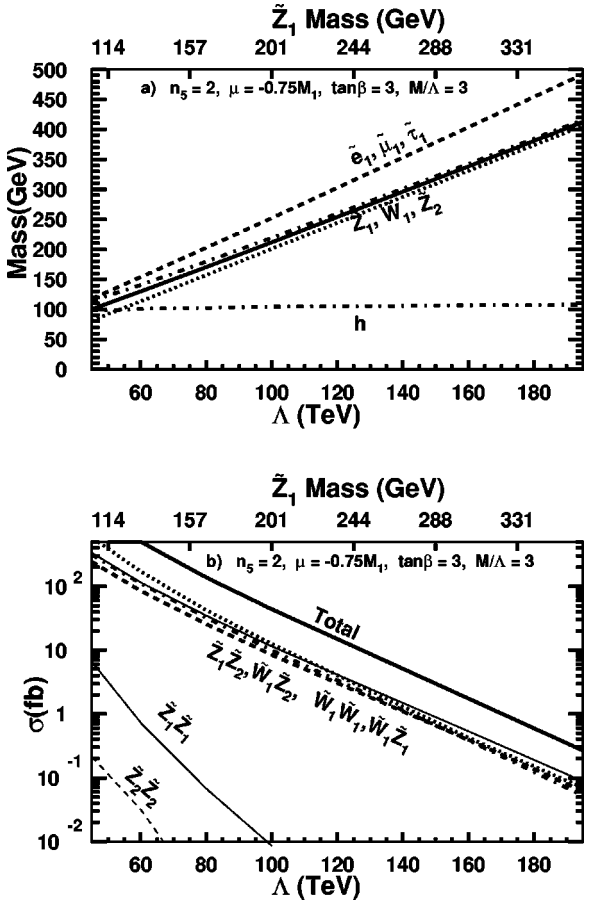

FIG. 13. The same as Fig. 2, but for the Higgsino NLSP model line D. In frame (a) the dotted line denotes the lightest neutralino, the solid line denotes the lighter chargino and the upper dot-dashed line denotes the second lightest neutralino. In frame (b) the dashed, dot-dashed, solid and dotted lines denote cross sections for $\tilde{Z}_1\tilde{Z}_2$, $\tilde{W}_1\tilde{Z}_2$, $\tilde{W}_1\tilde{W}_1$, $\tilde{W}_1\tilde{Z}_1$ production, respectively.

We see that at MI (TeV33) experiments should be able to probe Λ values out to about 80 TeV (90 TeV) corresponding to $m_{\tilde{W}_1} \sim 165$ GeV (180 GeV) via a search for $\gamma\gamma + \not{E}_T$ events.

For larger values of Λ, the NLSP dominantly decays via $\tilde{Z}_1 \rightarrow \tilde{G}h$ and the di-photon signal drops sharply. In this case, since h mainly decays via $h \rightarrow b\bar{b}$, the SUSY signal, which can contain up to four b-quarks, will be characterized by multiple tagged b-jet plus $\not{E}_T$ events, which may also contain other jets, leptons and possibly photons (if one of the NLSPs decays via the photon mode). The dominant SM background to multi-b events presumably comes from $t\bar{t}$ production and is shown in Table IV, where we have also shown the signal cross section for $\Lambda = 100$ TeV. For events with one or two tagged b-jets, the $t\bar{t}$ backgrounds come when the bs from t decay are tagged; i.e., the rate for events where other jets are mis-tagged as b's is just a few percent. This is also true for signal events. On the other hand, in the $3b$ channel, at least one of the tagged bs in the $t\bar{t}$ background has to come from a c or light quark or gluon jet that is misidentified as a b-jet, or from an additional b produced by QCD radiation. This is

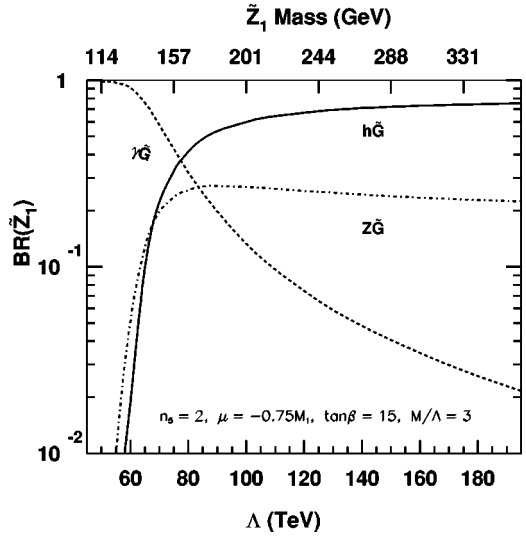

FIG. 14. Branching ratios for various decays of the neutralino NLSP versus Λ for model line D. The upper scale shows the neutralino mass.

not, however, the case for signal events which contain up to four b-jets. In each of the last two columns of Table IV where we show the top background and the SUSY signal, we present two numbers: the first of these is the cross section when all the tagged jets come from real b's, while the second number in parenthesis is the cross section including c and light quark or gluon jets that are mistagged as b. Indeed we see that the bulk of the $3b$ background is reducible and comes from mistagging jets, whereas the signal is essentially all from real bs.

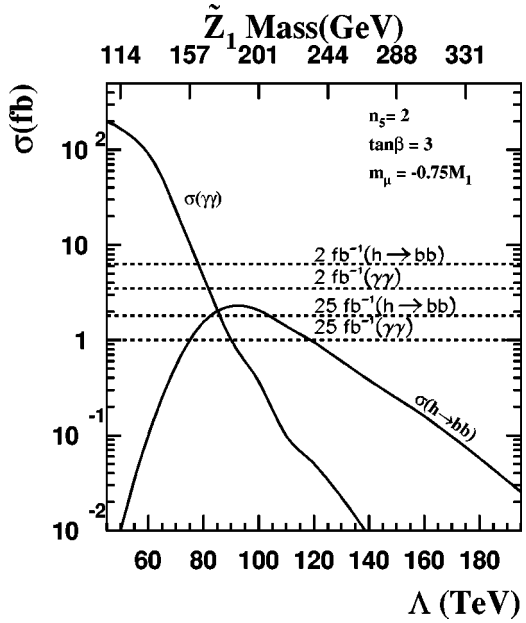

FIG. 15. SUSY signal cross sections for the inclusive $\gamma\gamma + \not{E}_T$ events [labelled $\sigma(\gamma\gamma)$], and for events with ≥ 3 tagged b-jets [labelled $\sigma(h \rightarrow bb)$] after all cuts described in the text for model line D. The dashed horizontal lines denote the minimum cross section for the signal to be observable at the 5σ level at the MI and at TeV33.

TABLE IV. The background cross section in fb for multiple tagged b-jets plus lepton plus $\not{E}_T$ events from $t\bar{t}$ production after basic cuts and triggers discussed in the text. Also shown are the corresponding SUSY signal cross sections for $\Lambda = 100$ TeV for model line D. The numbers in parentheses for the $3b$-channel include events from charm or light quark jets jets faking a b-jet. Whereas this fake rate dominates the background in the $3b$ channel, it is negligible in the $1b$ and $2b$ channels.

	$1b$		$2b$		$\geq 3b$	
	$t\bar{t}$	$\Lambda = 100$ TeV	$t\bar{t}$	$\Lambda = 100$ TeV	$t\bar{t}$	$\Lambda = 100$ TeV
$0l$	508	11.6	221	7.5	1.2 (8.1)	2.6 (2.7)
$1l$	812	1.2	345	0.57	1.5 (9.3)	0.11 (0.11)
$2l$	132	0.49	56	0.31	0.13 (0.31)	0.04 (0.05)
$3l$	0.22	0.03	0	0.04	0 (0)	0 (0)

It is clear from Table IV that the best signal to background ratio is obtained for events with $\geq 3b$-jets. Our detailed analysis shows that although the signal cross section is rather small, $3b$-channel with a lepton veto (since top events with large $\not{E}_T$ typically contain leptons) offers the best hope for identifying the signal above SM backgrounds. We see that the signal is of similar magnitude as the background for $\Lambda = 100$ TeV, a point beyond the reach via the $\gamma\gamma$ channel. To further enhance the signal relative to the background, we impose the additional cuts,

$\not{E}_T \geq 60$ GeV, and

60 GeV $\leq m_{bb} \leq 140$ GeV for at least one pair of tagged b-jets in the event.

The first of these reduces the signal from 2.7 fb to 2.1 fb, while the background is cut by more than half to 3.4 fb. The mass cut was motivated by the fact that in these models, at least one pair of tagged b's comes via $h \to bb$ decay, with $m_h \sim 100$ GeV, while the b's from top decay form a continuum. We found, however, that this cut leads to only a marginal improvement in the statistical significance and the signal to background ratio. We traced this to the fact that, because of top event kinematics, one b-pair is likely to fall in the ''Higgs mass window.'' Reducing this window to 100 ± 20 GeV leads to a slightly improved S/B, but leads to too much loss of signal to improve the significance.

The signal cross section via the $3b$ channel after the basic cuts as well as the additional $\not{E}_T$ and m_{bb} cuts introduced above is shown by the solid curve labeled $h \to bb$ in Fig. 15. For small values of Λ, the signal is small because of the reduction in the branching fraction for $\tilde{Z}_1 \to h\tilde{G}$ decay. The corresponding dashed lines shows the minimum cross section for a signal to be observable at the 5σ level at the MI and at TeV33. We see that, at the MI, there will be *no observable* signal in this channel. In fact, even for the Λ value corresponding to the largest signal, the statistical significance is barely 2σ, so that a non-observation of a signal will not even allow exclusion of this model line at the 95% C.L. With 25 fb^{-1} of integrated luminosity, the signal exceeds the 5σ level for 82 TeV $\leq \Lambda \leq 105$ TeV (corresponding to $m_{\tilde{W}_1} \sim m_{\tilde{Z}_1} \sim m_{\tilde{Z}_2} \sim 220$ GeV), and somewhat extends the reach obtained via the $\gamma\gamma$ channel. Furthermore, there appears to be no window between the upper limit of the $\gamma\gamma$ channel and the lower limit of the $3b$-channel. A few points are worth noting.

(1) Since the background dominantly comes from events where a c or light quark or gluon jet is mis-tagged as a b-jet, the reach via the $3b$ channel is very sensitive to our assumptions about the b mis-tag rate. Indeed, if the mis-tag rate is twice as big as we have assumed, there will be no reach in this channel even at TeV33.

(2) The $3b$ signal starts to become observable for $\Lambda \gtrsim 80$ TeV where the branching fraction for the decay $\tilde{Z}_1 \to h\tilde{G}$ becomes comparable to that for the decay $\tilde{Z}_1 \to \gamma\tilde{G}$. The value of Λ for which the Higgs decay of the neutralino becomes dominant depends on m_h, which in turn is sensitive to $\tan\beta$.

(3) Although we have not shown it here, signals involving b-jets together with additional photons or Z bosons identified via their leptonic decays have very small cross sections and appear unlikely to be detectable even for $\Lambda \sim 100$ TeV.

Despite the fact that the top background alone is 50 to several hundred times larger than the SUSY signal in all relevant one and two tagged b plus multilepton channels in Table IV, we have examined whether it was possible to separate the signal from the background. We focussed on the $2b + 0l$ signal which has the best S/B ratio, and required in addition that $\not{E}_T \geq 60$ GeV (which reduces the background by almost 50% with about a 20% loss of signal) and further 60 GeV $\leq m_{bb} \leq 140$ GeV (which reduces the background by another factor of half with a loss of 25% of the signal) [35]. We found, however, that the signal is below the 5σ level over essentially the entire range of Λ even at TeV33: only for $\Lambda = 80 \pm 5$ TeV does the signal cross section exceed this 5σ level of 7.7 fb. Moreover the S/B ratio never exceeds about 15% which falls below our detectability criterion $S/B \geq 20\%$. We found that while it is possible to improve the S/B ratio via additional cuts, these typically degrade the statistical significance of the signal. We thus conclude that for model line D, there will be no observable signal in the $2b$ channel even at TeV33.

Before closing this discussion, it seems worth noting that we should interpret the reach in Fig. 15 with some care, because unlike in the study of model lines A, B and C, we do not really have a well-motivated underlying theory (that gives a Higgsino NLSP). We realized this by arbitrarily taking $\mu = -\frac{3}{4}M_1$. The NLSP decay pattern, and hence the precise value of the reach, would depend on this choice which should be regarded as illustrative. In general, however, for

the Higgsino NLSP model line, the coupling of the NLSP to Higgs bosons is substantial so that the branching fraction for the decay $\tilde{Z}_1 \to h\tilde{G}$ becomes large when this decay is not kinematically suppressed. For small values of Λ, such that the NLSP can only decay via $\tilde{Z}_1 \to \gamma\tilde{G}$, SUSY signals should be readily observable in the $\gamma\gamma + \not{E}_T$ channel; once the NLSP decay to h begins to dominate, the cross section for diphoton events becomes unobservably small, and the SUSY signal mainly manifests itself as multiple b events which have large backgrounds from $t\bar{t}$ production. The most promising way to search for SUSY then seems to be via $\not{E}_T$ events with $\geqslant 3$ tagged b-jets, but for a search in this channel, an integrated luminosity of 25 fb^{-1} appears essential. A signal that extends the reach beyond that in the $\gamma\gamma$ channel is possible provided experiments are able to reduce the background from mis-tagged charm (light quark or gluon) jets to below 5% (0.2%).

IV. SUMMARY AND CONCLUDING REMARKS

The GMSB framework provides a phenomenologically viable alternative to the MSUGRA model. The novel feature of this framework is that SUSY breaking may be a low energy phenomenon. In this case, the gravitino is by far the lightest sparticle, and the NLSP decays within the detector into a gravitino and SM sparticles. Sparticle signals, and hence the reach of experimental facilities, are then sensitive to the identity of the NLSP.

In this paper, we have examined signals for supersymmetric particle production at the Fermilab Tevatron, and evaluated the SUSY reach of experiments at the MI or at the proposed TeV33 within the GMSB framework. In our study, we consider four different model lines, each of which lead to qualitatively different experimental signatures. We use the event generator to simulate experimental conditions at the Fermilab Tevatron, and for each model line, we have identified additional cuts that serve to enhance the SUSY signal over SM backgrounds. We assume the NLSP decay is prompt. This is a conservative assumption in that we do not make use of a displaced vertex to enhance the signal over SM background.

For the first of these model lines, labeled A, the NLSP is mainly a hypercharge gaugino and dominantly decays via $\tilde{Z}_1 \to \tilde{G}\gamma$, so that SUSY will lead to extremely striking events with multiple jets with hard leptons and large $\not{E}_T$ and up to two hard, isolated photons, with cross sections (after all cuts) shown in Fig. 4. The physics background to the $\gamma\gamma$ event topologies is very small, and detector-dependent instrumental backgrounds (such as from jets being misidentified as photons or leptons, or large mismeasurement of transverse energies) dominate [30]. Even with a conservative estimate of 1 fb for the background cross section, experiments at the MI (TeV33) should be able to probe values of the model parameter Λ out to 110 TeV (130 TeV). If we optimistically assume that this background can be reduced to a negligible level by hardening the cuts on the photons and $\not{E}_T$, we find a reach as high as $\Lambda \sim 118$ TeV (corresponding to a gluino of 950 GeV) at the MI and of 145 TeV at TeV33. For this model line, the $ll\gamma\gamma + \not{E}_T$ signal from slepton pair production may be observable at TeV33 even if sleptons are as heavy as 180 GeV.

In model line B, the lighter stau is the NLSP, and heavier sparticles cascade decayed down to the stau, which then decays via $\tilde{\tau}_1 \to \tau\tilde{G}$. The presence of isolated tau leptons [9], in addition to jets and other leptons is the hallmark of such a scenario. We found, however, that in some channels, the background from misidentification of QCD jets as τ completely swamp the physics backgrounds, making it very difficult to detect the signal (see, e.g., the $C1\tau 1l$ channel in Table I) in this channel. We conclude that unless τ misidentification can be greatly reduced from what we have assumed, SUSY will only be detectable via channels with at least three leptons (e, μ and τ) for which the cross sections are individually small, and then, only by summing the signal in several channels. Even here, backgrounds from misidentified taus are significant. Our assessment of the reach is shown in Fig. 8. We see that at the MI, the clean multilepton channel offers the best reach, out to $\Lambda = 42$ GeV (corresponding to $m_{\tilde{W}_1} = 192$ GeV and squarks and gluinos as heavy as 700 GeV), while at TeV33, the reach may be extended out to Λ values somewhat beyond 50 TeV ($m_{\tilde{g}} \sim 800$ GeV).

In model line C, the lighter stau is again the NLSP, but the lighter selectron and smuon are essentially degenerate with it, so that $\tilde{e}_1$ and $\tilde{\mu}_1$ cannot decay into a tau; i.e., these decay into a gravitino and a corresponding lepton. Since cascade decays of sparticles are equally likely to terminate in each flavor of slepton, we expect that this model line will lead to very large multiplicities of e, μ and τ in SUSY events. Indeed we found that the optimal strategy in this case was to search for events with $n_e + n_\mu \geqslant 4$ or $n_e + n_\mu + n_\tau \geqslant 4$ with $n_e + n_\mu \geqslant 2$. The reach is shown in Fig. 12. We see that at the MI, there should be observable signals out to $\Lambda = 45$ TeV, while at TeV33 Λ values as high as 55 TeV should be observable. These correspond to a gluino (chargino) mass of 1000 (320) GeV and 1200 (400) GeV, respectively.

Finally, we have examined an unorthodox model line where, by hand, we adjust the value of μ to be smaller than the value of the hypercharge gaugino mass M_1. This leads to an NLSP which is dominantly a Higgsino. Furthermore, $m_{\tilde{W}_1} \sim m_{\tilde{Z}_2} \sim m_{\tilde{Z}_1}$ so that the fermions from $\tilde{W}_1$ and $\tilde{Z}_2$ decays to $\tilde{Z}_1$ are soft, and SUSY event topologies are largely determined by the decay pattern of $\tilde{Z}_1$. For small values of Λ for which the NLSP can only decay via $\tilde{Z}_1 \to \gamma\tilde{G}$, the signal is readily observable in the $\gamma\gamma + \not{E}_T$ channel. However, once the NLSP decay to h begins to dominate, SUSY mainly manifests itself as multiple b events which have large backgrounds from $t\bar{t}$ production. The most promising way to search for SUSY then seems to be via $\not{E}_T$ events with $\geqslant 3$ tagged b-jets and zero leptons. For a search in this channel, an integrated luminosity of ~ 25 fb^{-1} appears essential. A signal that extends the reach beyond that in the $\gamma\gamma$ channel is possible provided experiments are able to reduce the background from mis-tagged charm (light quark or gluon) jets to

below 5% (0.2%). The reach for model line D is shown in Fig. 15, but it should be kept in mind that the details of this figure will be sensitive to our assumption about μ.

To conclude, in GMSB models signals for SUSY events will be quantitatively and qualitatively different from those in the MSUGRA framework. This is primarily because a neutralino NLSP decays into a photon, a Z boson or a Higgs boson and a gravitino, or sparticles cascade decay to a slepton NLSP which decays to leptons and a gravitino: these additional bosons (or their visible decay products), or leptons from slepton NLSP decays, often provide an additional handle which may be used to enhance the signal over SM background. Although we have not performed an exhaustive parameter scan, for the model lines that we studied, we found that the SUSY reach (as measured in terms of the mass of the dominantly produced sparticles) is at least as big, and frequently larger than in the MSUGRA framework. For some cases, this conclusion depends on the capability of experiments to identify τ leptons and b-quarks with moderately high efficiency and purity. In view of the diversity of signals that appear possible for just this one class of models, we encourage our experimental colleagues to be in readiness for tagging third generation particles as they embark on the search for new phenomena in run II of the Tevatron.

ACKNOWLEDGMENTS

We are grateful to our colleagues in the gauge-mediated SUSY breaking group of the run II SUSY and Higgs Workshop, especially Steve Martin, Scott Thomas, Ray Culbertson and Jianming Qian for sharing their insights. Model lines I and II were first studied at this Workshop. We thank Regina Demina for her guidance on b-jet tagging and mistagging efficiencies. P.M. was partially supported by Fundação de Amparo à Pesquisa do Estado de São Paulo (FAPESP). This research was supported in part by the U.S. Department of Energy under Contract No. DE-FG02-97ER41022 and DE-FG-03-94ER40833.

[1] M. Dine, W. Fischler, and M. Srednicki, Nucl. Phys. **B189**, 575 (1981); S. Dimopoulos and S. Raby, *ibid.* **B192**, 353 (1981); L. Alvarez-Guamé, M. Claudson, and M. Wise, *ibid.* **B207**, 96 (1982).

[2] M. Dine and A. Nelson, Phys. Rev. D **48**, 1277 (1993); M. Dine, A. Nelson, and Y. Shirman, *ibid.* **51**, 1362 (1995); M. Dine, A. Nelson, Y. Nir, and Y. Shirman, *ibid.* **53**, 2658 (1996).

[3] S. Dimopoulos, M. Dine, S. Raby, and S. Thomas, Phys. Rev. Lett. **76**, 3494 (1996); S. Dimopoulos, S. Thomas, and J. Wells, Phys. Rev. D **54**, 3283 (1996); Nucl. Phys. **B488**, 39 (1997).

[4] S. Ambrosanio *et al.*, Phys. Rev. Lett. **76**, 3498 (1996); Phys. Rev. D **54**, 5395 (1996).

[5] K. S. Babu, C. Kolda, and F. Wilczek, Phys. Rev. Lett. **77**, 3070 (1996).

[6] H. Baer, M. Brhlik, C. H. Chen, and X. Tata, Phys. Rev. D **55**, 4463 (1997).

[7] J. Bagger, K. Matchev, and D. Pierce, Phys. Rev. D **55**, 3188 (1997).

[8] R. Rattazzi and U. Sarid, Nucl. Phys. **B501**, 297 (1997).

[9] D. Dicus, B. Dutta, and S. Nandi, Phys. Rev. Lett. **78**, 3055 (1997); Phys. Rev. D **56**, 5748 (1997); K. Cheung, D. Dicus, B. Dutta, and S. Nandi, *ibid.* **58**, 015008 (1998); B. Dutta, D. J. Mueller, and S. Nandi, Nucl. Phys. **B544**, 451 (1999); D. J. Mueller and S. Nandi, Phys. Rev. D **60**, 015008 (1999).

[10] C. H. Chen and J. F. Gunion, Phys. Lett. B **420**, 77 (1998); Phys. Rev. D **58**, 075005 (1998).

[11] J. Feng and T. Moroi, Phys. Rev. D **58**, 035001 (1998).

[12] E. Gabrielli and U. Sarid, Phys. Rev. D **58**, 115003 (1998).

[13] H. Baer, P. G. Mercadante, X. Tata, and Y. Wang, Phys. Lett. B **435**, 109 (1998).

[14] S. Martin and J. Wells, Phys. Rev. D **59**, 035008 (1999).

[15] See G. Giudice and R. Rattazzi, hep-ph/9801271, 1998 for a review.

[16] For a review of the MSUGRA model, see H. P. Nilles, Phys. Rep. **110**, 1 (1984); R. Arnowitt and P. Nath, Lectures presented at the VII J. A. Swieca Summer School, Campos do Jordao, Brazil, 1993, Report No. CTP-TAMU-52/93.

[17] S. Martin, Phys. Rev. D **55**, 3177 (1997).

[18] N. Deshpande, B. Dutta, and S. Oh, Phys. Rev. D **56**, 519 (1997).

[19] M. S. Alam *et al.*, Phys. Rev. Lett. **74**, 2885 (1995); R. Barate *et al.*, Phys. Lett. B **429**, 169 (1998).

[20] ALEPH Collaboration, R. Barate *et al.*, Phys. Lett. B **429**, 201 (1998); DELPHI Collaboration report at the LEP Experiments Committee Meeting, CERN, 1998; see also, P. Abreu *et al.*, Eur. Phys. J. C **7**, 595 (1999); L3 Collaboration, M. Acciari *et al.*, Phys. Lett. B **444**, 503 (1998).

[21] The limit $m_{\tilde{W}_1} \gtrsim 150$ GeV from a non-observation [30,31] of an excess in diphoton $+\not{E}_T$ events at the Tevatron translates to a bound $m_{\tilde{Z}_1} \gtrsim 72$ GeV and independently excludes a slightly smaller region of the plane.

[22] L3 Collaboration report at the LEP Experiments Committee Meeting, CERN, 1998. See also reports of other collaborations.

[23] We are grateful to Graham Kribs, Steve Martin and Jim Wells for bringing this to our attention.

[24] H. Baer, F. Paige, S. Protopopescu, and X. Tata, hep-ph/9810440, 1998.

[25] S. Ambrosanio, S. Martin, and G. Kribs, Nucl. Phys. **B516**, 55 (1998).

[26] In addition to these decays, ISAJET also includes several other three body decays of $\tilde{l}_2 \simeq \tilde{l}_L, \tilde{\tau}_2$ and $\tilde{\nu}_l, \tilde{\nu}_\tau$ in various approximations. These decays are unimportant for us because the heavier sleptons generally have two-body decays, but might be important in models [28] where these are light. The reader who uses ISAJET in models where these decays are important is advised to become aware of the various approximations under which these are calculated.

[27] S. Dimopoulos, Thomas, and Wells, Ref. [3].

[28] This is not special to GMSB models. It could happen in models with additional *D*-terms which invert the customary hierarchy between left- and right- sleptons. See, e.g., J. Amundson *et al.,* in New Directions for High Energy Physics, Snowmass, CO, 1996, edited by D. Cassel, L. Trindle Gennari and R. Siemann; A. de Gouvea, A. Friedland, and H. Murayama, Phys. Rev. D **59**, 095008 (1999); for examples of such terms in the SUGRA framework (where the inversion is easier than in the GMSB model, since sleptons start out with universal masses).

[29] These model lines were first proposed for study at the run II SUSY and Higgs Workshop held at Fermilab in 1998. The nomenclature used is different from that in the Workshop.

[30] B. Abbott *et al.,* Phys. Rev. Lett. **80**, 442 (1998).

[31] F. Abe *et al.,* Phys. Rev. Lett. **81**, 1791 (1998); Phys. Rev. D **59**, 092002 (1999).

[32] Although the chargino pair production cross section is an order of magnitude larger than the slepton cross section, it should be remembered that the branching fraction for both charginos to decay to e or to μ is just $\sim 2\%$.

[33] Admittedly, we have not attempted to separate slepton events from other SUSY sources. These additional SUSY sources dominate for $\Lambda \leqslant 90$ GeV for which $\tilde{Z}_2 \rightarrow l\tilde{l}_1$ is kinematically accessible and has a large branching ratio. Lepton pairs from neutralino decays will necessarily have $m(ll) \leqslant m_{\tilde{Z}_2}\sqrt{1-m^2_{\tilde{l}_1}/m^2_{\tilde{Z}_2}}\sqrt{1-m^2_{\tilde{Z}_1}/m^2_{\tilde{l}_1}}$, while those from slepton pair production form a continuum, possibly extending beyond this.

[34] We have checked that this additional requirement causes essentially no loss of signal.

[35] We studied several other distributions including, jet multiplicity, θ_{bb}, $\delta\phi(bb)$, but none of these proved useful to enhance the signal over the top background.

[36] M. Hohlmann, Report No. Fermilab-Conf-96/330-E, 1996.